

# Microcavity Plasma Devices and Arrays Fabricated by Plastic-Based Replica Molding

Meng Lu, *Student Member, IEEE*, Sung-Jin Park, *Member, IEEE*, Brian T. Cunningham, *Member, IEEE*, and J. Gary Eden, *Fellow, IEEE*

**Abstract**—The fabrication of lightweight and optically transparent arrays of microplasma devices having microcavities fabricated by a polymer-based replica molding process is reported. This process enables arrays of microcavity plasma devices and connecting channels with feature sizes as small as  $20\ \mu\text{m}$  to be produced inexpensively and precisely over surface areas of at least tens of square centimeters. Devices having transparent electrodes and substrates (including glass and flexible plastic) have been operated successfully at rare gas pressures up to 700 torr. Individual microplasma pixels with cross-sectional dimensions of  $200 \times 200\ \mu\text{m}^2$  and  $50 \times 50\ \mu\text{m}^2$ , as well as plasma channels having widths of 20 and  $150\ \mu\text{m}$  and aspect ratios (channel length : width) as large as  $10^4 : 1$ , have been fabricated and tested. Representative voltage–current data for these structures and lifetime measurements for a  $20 \times 20$  pixel array are presented. [2006-0099]

**Index Terms**—Flexible display, microcavity plasmas, replication process, transparent display.

## I. INTRODUCTION

MICROPLASMAS have been studied for more than four decades in several contexts, the best known of which is as the source of incoherent vacuum ultraviolet (VUV) radiation for plasma display panels [1]. Recently, however, the spatial confinement of a low-temperature nonequilibrium plasma to a microcavity has been demonstrated to yield a unique class of photonic/electronic devices and open new avenues in plasma science and technology [2]. Having a characteristic dimension  $d$  below nominally  $500\ \mu\text{m}$ , microcavity plasma devices are capable of producing radiation from atomic and molecular species over an extraordinarily broad spectral region (extreme ultraviolet to far infrared). Furthermore, the physical processes governing the operation of these devices can differ from those for conventional macroscopic devices [3], resulting in the formation and steady-state operation of stable glow discharges at pressures up to one atmosphere and beyond [4]. Such devices have been fabricated from a wide range of substrates, dielectric materials, and electrode configurations, and structures with  $d$  as small as  $10\ \mu\text{m}$  (and plasma volumes in the nanoliter range)

have operated successfully in the rare gases [5]. Recent advances in the development of ultralarge arrays of microplasma devices include the demonstration of arrays comprising 250 000 ( $500 \times 500$ ) devices having microcavities in the form of an inverted square pyramid [6]. Though still in its infancy, it is clear that this technology is promising for several commercial applications, including displays, analytical spectroscopy [7], medical phototherapy (photodynamic therapy), biological sterilization, UV curing (photopolymerization), and integrated photonic circuit light sources.

Although several microcavity plasma structures that are flexible have been reported [8]–[10], a fully transparent design has not yet been developed. This paper describes the fabrication of microplasma devices and arrays by a replica molding process in which the substrate is flexible and transparent plastic film or glass. Capable of accurately producing high aspect ratio (channel length:width  $10^3 : 1$ ) cavities with lateral dimensions ( $d$ ) approaching  $1\ \mu\text{m}$ , this approach is inexpensive and scalable to processing surface areas beyond  $10^2\ \text{cm}^2$ . Single devices and arrays as large as 400 pixels ( $20 \times 20$ ) have been demonstrated to date, and the following sections describe measurements of several of their electrical and optical characteristics.

## II. DEVICE DESIGN AND FABRICATION

The design and fabrication of the devices reported here is based upon replication of the microplasma cavity in a transparent polymer material through a molding process. The surface of the mold is a negative volume profile of the desired microcavity shape, and the mold itself is either flexible or rigid, depending on whether the substrate is rigid or flexible, respectively. Replicating the mold shape in a liquid polymer material that can be cured by exposure to UV radiation yields a cavity formation process that is inexpensive and amenable to mass production but is also capable of producing cavities with depths of tens of micrometers without the need for large forces or high temperatures, such as those generally required with stamping approaches. Perhaps more importantly, channels with transverse dimensions approaching  $1\ \mu\text{m}$  and aspect ratios  $> 10^3 : 1$  can now be produced.

### A. Device Structure

A cross-sectional diagram of a representative microplasma device fabricated in transparent materials is shown in Fig. 1. The substrate is either a rigid sheet of glass or a flexible polyester (PET) film coated with a conducting thin film of indium tin oxide (ITO). The ITO film constitutes the bottom electrode of the device and, in this design, is common to all of the devices in an array. The microplasma cavities are formed in a layer of

Manuscript received May 26, 2006; revised August 13, 2006. This work was supported by the U.S. Air Force Office of Scientific Research under Grant F49620-03-1-0391 Subject Editor N. de Rooij.

The authors are with the Department of Electrical and Computer Engineering, University of Illinois at Urbana-Champaign, Urbana, IL 61801 USA (e-mail: bcunning@uiuc.edu).

Color versions of Figs. 1–4, 7, and 8 are available online at <http://ieeexplore.ieee.org>.

Digital Object Identifier 10.1109/JMEMS.2006.886034

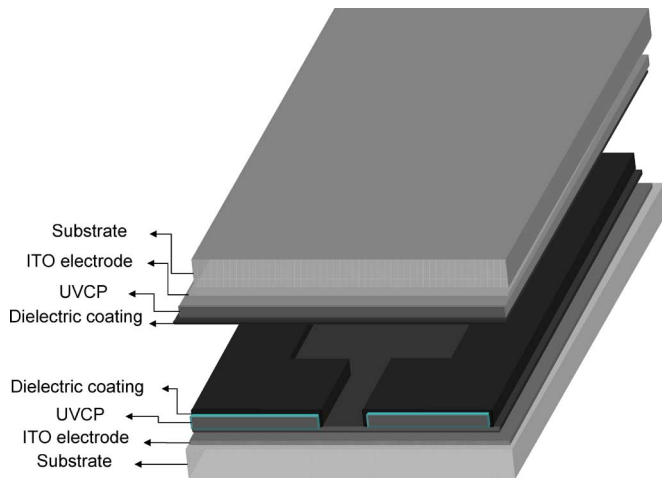


Fig. 1. Generalized diagram of a microcavity plasma structure fabricated by a replica molding process with UV-cured polymer (UVCP).

UV-curable polymer by a replica molding process, in which the depth of the UV-curable polymer layer must slightly exceed that for the desired plasma cavity. Following the cavity replication process, the cavities may be coated with a dielectric material, such as titanium dioxide, silicon dioxide, tantalum oxide, magnesium oxide, or silicon nitride, which serves to protect the polymer cavity from exposure to the plasma. Ions accelerated in the sheath region of the plasma, in the direction of the temporal cathode, can attain energies of hundreds of eV and are frequently responsible for the degradation of plasma devices in which the electrodes are exposed directly to the plasma. The dielectric material also serves as a barrier against organic vapors (from the cured polymer) entering the sealed plasma cavity. Another potential function of the dielectric (and MgO, in particular) is to provide supplemental electrons to the plasma by secondary emission.

The upper electrode in Fig. 1 is an ITO-coated cover substrate that is bonded to the top of the polymer cavity. Prior to bonding, the cover may also be coated with a thin film for dielectric passivation purposes. In the work reported here, the upper ITO electrode was not patterned to selectively energize individual pixels and is, therefore, also common to all the pixels in an array. Narrow channels (typically  $20 \times 20 \mu\text{m}^2$  in cross-section) that extend to the edge of the finished device are also integrated into the structure of Fig. 1 for the purpose of evacuating and backfilling the device or array. After bonding the cover to the lower portion of the structure, electrical leads are attached to the upper and lower electrodes to enable operation of the device. Before leaving this section, it should be noted that, owing to their locations in the structure of Fig. 1, the dielectric barrier films will contribute to the overall capacitance of the device or array. Patterning one or both of the films will mitigate this effect and improve the high-frequency characteristics of the device.

### B. Fabrication Process

We begin by describing the procedure for fabricating microplasma devices on a rigid ITO-coated glass substrate. Because separation of the mold from the workpiece is facilitated

by choosing *either* the mold or the workpiece to be mechanically flexible, device fabrication on a rigid glass substrate is facilitated by the use of a flexible mold. A polydimethylsiloxane (PDMS, DuPont Sylgard 184) silicone elastomer mold with a negative volume profile of the desired microcavity surface structure was produced by first fabricating a silicon “master” wafer with a positive volume image of the microcavities. Details of the fabrication process are illustrated in Fig. 2. The master pattern was produced on a 4-in-diameter Si wafer by conventional photolithography to define the cavity regions. After photoresist development, the cavity patterns were etched to a depth of  $80 \mu\text{m}$  by inductively coupled plasma (ICP) reactive ion etching (RIE) with the Bosch process (Surface Technology Systems). Gas channel patterns were produced in the silicon master wafer through alignment and photolithographic patterning with a second mask, followed by etching the channel pattern by ICP-RIE to a depth of  $20 \mu\text{m}$ . Using a single silicon master, PDMS “daughter” molds were produced by setting an aluminum ring over the silicon wafer and pouring 40 g of a PDMS elastomer:curing agent mixture (1:10) into the ring. The 4-mm-thick PDMS mold was thermally cured ( $110^\circ\text{C}$ , 4 h) and then peeled from the silicon master.

To fabricate the microcavity array, a layer of liquid, UV-curable polymer material (Type SK-9, Summers Inc.) was squeezed between the PDMS mold and the ITO-coated glass substrate. At room temperature, the viscosity of the liquid UV-curable polymer is  $\sim 80$  cps, resulting in no air bubble formation when the PDMS mold is gradually placed from one end of the replica to the other. The liquid, UV-curable polymer was allowed to flow into the mold shape, and subsequently was exposed to UV illumination which results in curing of the polymer. The viscosity of the liquid, UV-curable polymer is selected so as to enable rapid filling of the mold shape without the application of substantial force between the mold and the substrate. The UV-curing process takes place at room temperature and occurs in  $\sim 10$ – $90$  s, depending on the polymer material, the curing initiation agent, and the desired degree of curing. The result is a thin ( $5 \mu\text{m}$ ) base layer of cured polymer between the bottom of the mold and the surface of the ITO bottom electrode, in which the base layer thickness is controlled by the liquid polymer viscosity, the temperature of the replication process, and the pressure applied between the substrate and the mold during replication. The base layer protects the bottom electrode from exposure to the discharge and is another component of the system that contributes to the device capacitance. After curing, the PDMS mold and the replica of the microcavity device or array are separated by peeling the flexible mold away from the rigid substrate such that the cured polymer preferentially and permanently adheres to the substrate. Separation is facilitated by pretreatment of the mold with an antiadhesion monolayer coating, such as Repel Silane (Amersham Biosciences), or by evaporation of a thin metal film (such as gold, silver, or nickel) onto the mold surface. While a PDMS-based mold process is described here, the daughter mold may also be fabricated from flexible metal foil or plastic film. For a flexible substrate, such as ITO-coated polyethylene (PET) film, fabrication proceeds in a manner similar to the method described above, but a PDMS daughter mold is not necessary. Therefore, the silicon master contains a neg-

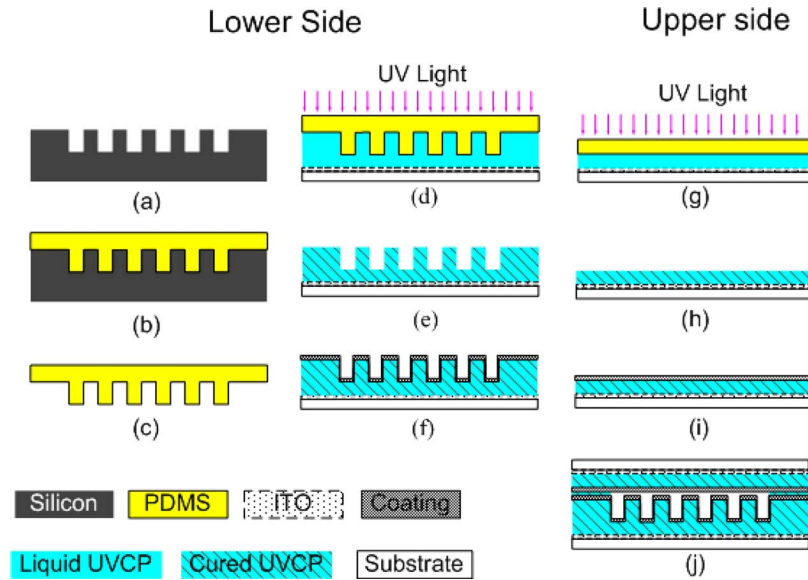


Fig. 2. Schematic diagram of the array fabrication procedure: (a) the process begins with a silicon master wafer produced by conventional photolithography and ICP-DRIE etching; (b) liquid PDMS is poured onto the silicon master wafer; (c) heat cured PDMS is peeled off; (d) liquid UV cured polymer is dispensed onto the substrate (glass or PET) and cured by UV illumination; (e) the cured structure is separated from PDMS; (f) dielectric film is deposited; (g) planar PDMS is used to make UV-cured polymer layer on upper part; (h) the PDMS is peeled off; (i) dielectric coating; and (j) two individual parts are bonded.

ative image of the desired surface structure pattern and is used directly for the fabrication of devices.

Capable of accurately reproducing feature sizes over a large range (tens of nanometers to hundreds of micrometers) [11], [12], the replica molding process reported here is well suited for mass production. We have previously demonstrated a similar process sequence for the fabrication of photonic crystal optical biosensors on continuous sheets of plastic film in a roll-to-roll fashion [13]. Consequently, it appears that the replica molding process outlined above is readily adaptable to the manufacture of arrays of microcavity plasma devices at production rates up to meters per minute.

Subsequent to replica molding, a dielectric thin film can be deposited over the cavity structure as a barrier layer. In the experiments conducted to date, devices having no dielectric, 500 nm of  $\text{SiO}_2$ , or 500 nm of  $\text{TiO}_2$  deposited by electron-beam evaporation (Temescal FC-1800) were studied.

As shown in Fig. 2(g)–(i), a planar layer of UV-curable polymer is replicated on the ITO-coated substrate with a flat PDMS mold, and a 500-nm-thick film of either  $\text{SiO}_2$  or  $\text{TiO}_2$  is deposited on the cover prior to attachment in order to isolate the polymer from the plasma environment. As mentioned previously, a cover comprising an ITO-coated transparent substrate (either glass or flexible PET film) is bonded to the replicated cavity structure. The cover was attached by spin-coating a thin (500 nm) layer of UV-curable adhesive onto the cover substrate, removing the adhesive in the device region, placing the cover against the replicated cavity structure, and completely curing the adhesive by exposure to ultraviolet for at least 90 s.

### C. Experimental Details

The completed microcavity plasma device or array structures of Fig. 1 were loaded into a vacuum chamber, evacuated to  $10^{-6}$  torr, and backfilled with research grade rare gases. All experiments involved driving the arrays with a sinusoidal or

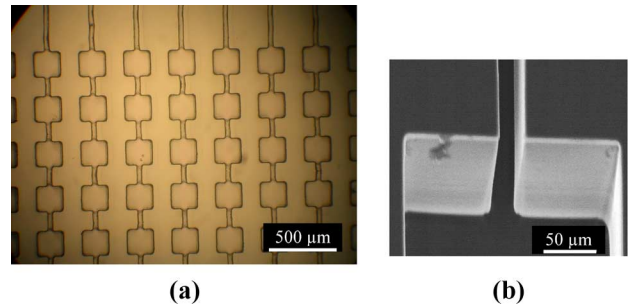


Fig. 3. (a) Optical micrograph of a  $7 \times 5$  segment of a  $20 \times 20$  array of microplasma devices. Each cavity has a  $200 \times 200 \mu\text{m}^2$  cross-section, and the gas flow (connection) channels are  $\sim 20 \mu\text{m}$  in width. (b) SEM image of the cross-section of a single cavity having a depth of  $76 \mu\text{m}$ .

bipolar dc voltage waveform, and current measurements were facilitated by a  $3.1 \text{ k}\Omega$  series resistor. Emission spectra were recorded with a 0.14 m spectrograph coupled to a charge-coupled device (CCD) array and having a resolution in first order of 0.4 nm.

### III. CHARACTERIZATION OF ARRAYS OF MICROCAVITY DEVICES

Several experiments were conducted to characterize the electrical, optical, and lifetime properties of  $20 \times 20$  arrays of microplasma devices. The production of stable glows in gas flow channels having widths as small as  $20 \mu\text{m}$  is also reported. Fig. 3(a) is an optical micrograph of a  $7 \times 5$  portion of a  $20 \times 20$  array of devices with microcavities  $200 \times 200 \mu\text{m}^2$  in cross-section and having a depth of  $76 \mu\text{m}$ . The interconnecting gas channels for this array have widths of  $\sim 20 \mu\text{m}$ . A scanning electron microscope (SEM) image of the cross-section of a single microcavity is presented in Fig. 3(b). It is evident from the micrograph that the walls of both the microcavity and gas channel are free from debris and essentially vertical. A vivid illustration of the transparency of these arrays is provided by Fig. 4, which comprises two photographs of a  $20 \times 20$  array,



Fig. 4. Photograph of a  $20 \times 20$  array of microplasma cavities situated between a U.S. one dollar bill and the camera: (a) the image before ignition of the array and (b) CCD image with device operated at a Ne pressure of 700 torr and an rms voltage of 340 V.

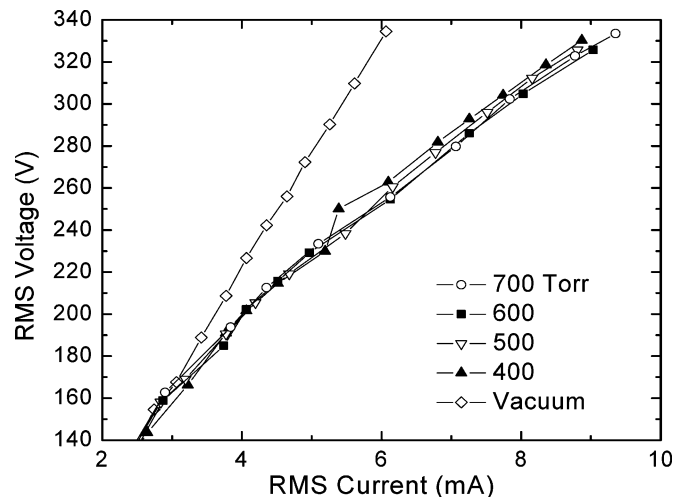


Fig. 5. V-I characteristics for a  $20 \times 20$  array of microcavities. The array is operated in Ne at pressures ranging from 400 to 700 torr, and the driving voltage is sinusoidal with a frequency of 20 kHz.

both of which were recorded with a U.S. dollar located behind the array. For the left-hand image of Fig. 4, the array is neither ignited nor visible. Once ignited for  $p_{\text{Ne}} = 700$  torr, however, the array (and the gas flow channels for the applied voltage of Fig. 4(b)— $V_{\text{RMS}} = 340$  V) is quite bright and the emission intensity is uniform from pixel-to-pixel.

Voltage-current (V-I) characteristics for a  $20 \times 20$  array of microcavity plasma devices having the structure of Fig. 2 are presented in Fig. 5. Data are given for operation in Ne at pressures between 400 and 700 torr when the array is driven by a sinusoidal voltage with a frequency of 20 kHz. The vacuum characteristic of the array is also given, and it is evident that the microplasmas are operating in the abnormal glow mode. Ignition of the array occurs for a root mean square (rms) voltage of  $170 \pm 3$  V and the lowest voltage at which the entire array is operational is  $\sim 145$  V rms. As noted above, the slope of the characteristic is positive irrespective of  $p_{\text{Ne}}$ , confirming that the array can be operated without the need for ballast, which is a substantial asset for commercial applications. Notice, too, that the characteristic varies little with increasing rare gas pressure. The slight decrease in voltage for a fixed value of operating current is a property of microplasma arrays observed previously at pressures approaching 1 atm [4].

Microplasma array lifetime has also been measured for several device designs, and the results are summarized in Fig. 6. Specifically, tests were conducted with three  $20 \times 20$  arrays

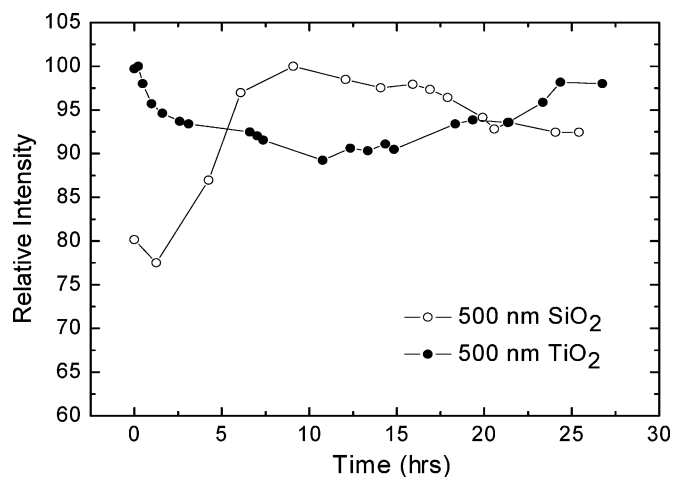


Fig. 6. Variation of the wavelength-integrated emission intensity from  $20 \times 20$  arrays over a  $\sim 26$  h time period. Data are shown for device structures in which the dielectric is a 500-nm-thick film of  $\text{SiO}_2$  ( $\circ$ ) or  $\text{TiO}_2$  ( $\bullet$ ). All data were acquired with an rms driving voltage and frequency of 248 V and 20 kHz, respectively, and the Ne pressure fixed at 700 torr.

having similar device structures but different dielectrics. One was fabricated with no dielectric, whereas the other two arrays incorporated a 500-nm-thick film of either  $\text{SiO}_2$  or  $\text{TiO}_2$ . The variation of the relative, wavelength-integrated emission intensity over a  $\sim 26$  h period is shown in Fig. 6 for the  $\text{SiO}_2$  and  $\text{TiO}_2$  dielectric structures. All of the data were recorded for an rms driving voltage and frequency of 248 V and 20 kHz, respectively, and the Ne pressure held constant at 700 torr. Although these results must be regarded as preliminary, the behavior of the arrays is observed to differ considerably between the three array designs. The radiative output of the  $\text{TiO}_2$ -based microcavity structure declines monotonically over the first 10–11 h of operation and slowly recovers thereafter. At 24 h, the emission intensity of this array has risen to within  $\sim 2\%$  of its initial value. In contrast, the visible emission generated by the microplasma device structure with the  $\text{SiO}_2$  dielectric *increases* by  $>20\%$  in the early stages of the test, peaks at  $\sim 9$  h, and subsequently declines. We attribute these results to two factors—the permeability of the respective dielectric films to organic species evolving from the polymer and the degree of hydrogen incorporation into the films during the deposition process—but further spectroscopic and surface analytical tests are necessary to unambiguously identify the physical mechanisms responsible for the divergent behavior of Fig. 6. Nevertheless, it is clear from the data that protecting the plasma microcavity with a dielectric barrier is essential for array longevity. Although the uncoated (i.e., no dielectric) structure survived for 24 h, serious degradation of the unprotected polymer cavities and channels became evident quickly, and Fig. 7(a) is a microphotograph of a portion of the  $20 \times 20$  array following a 24 h test. Discoloration of the structure and widening of the gas flow channels owing to plasma erosion of the polymer are obvious. In contrast, the array with the 500 nm  $\text{SiO}_2$  dielectric film emerged unscathed from the 24 h test, as illustrated by the optical micrograph on the right side of Fig. 7. It should be emphasized that the test conditions were identical for both arrays, and the structure of the dielectric is a critical factor in determining the array lifetime.

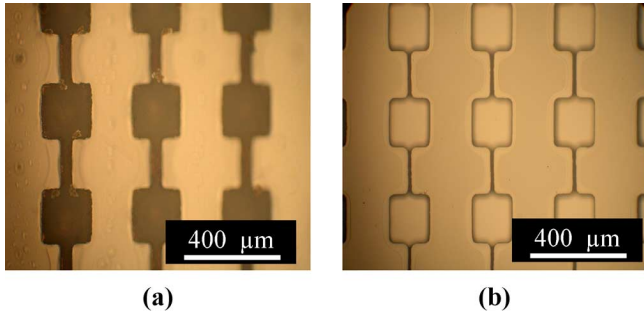


Fig. 7. Optical micrographs of portions of  $20 \times 20$  arrays after 24 h of continuous operation: (a) device structure with no dielectric and (b) device structure incorporating a 500-nm-thick  $\text{SiO}_2$  dielectric barrier. The operating conditions for both arrays were identical throughout the test ( $V_{\text{RMS}} = 248 \text{ V}$ , 20 kHz driving voltage,  $p_{\text{Ne}} = 700 \text{ torr}$ ).

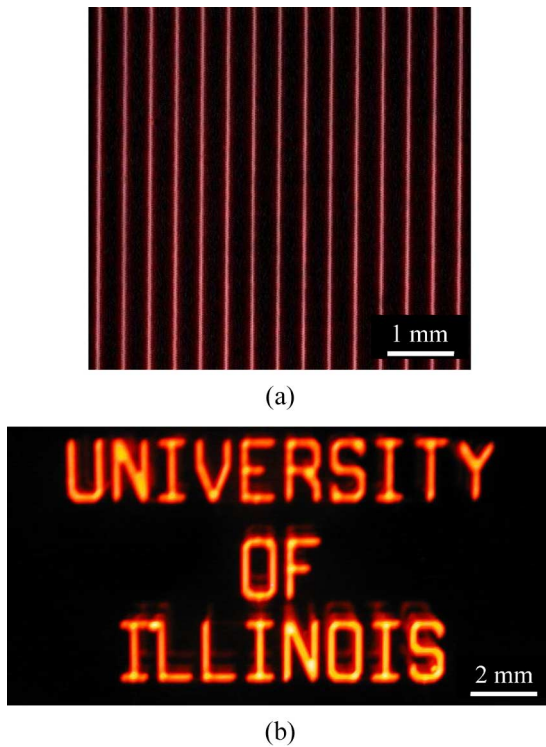


Fig. 8. Microphotographs of (a) an array of linear plasma channels having individual widths of  $20 \mu\text{m}$  and (b) a pattern of letters fabricated in  $200\text{-}\mu\text{m}$ -wide channels. Both arrays are operated in 700 torr of Ne with an rms voltage (20 kHz) of 248 V.

Experiments have also shown that diffuse, stable microplasmas can now be produced in channels as narrow as  $20 \mu\text{m}$  in width. Fig. 8(a) is a microphotograph of an array of linear microplasmas generated in 700 torr of Ne in  $20\text{-}\mu\text{m}$ -wide channels. To date, plasma channels with an aspect ratio as large as  $10^4 : 1$  have been realized. Having a channel width of  $100 \mu\text{m}$  and a (folded) length of 1 m, these plasma channels are diffuse glow discharges that are capable of continuous operation. We note that such an aspect ratio for a stable, reproducible plasma is unprecedented and long thought to not be possible on this spatial scale. For comparison, the aspect ratio for the low pressure plasma in a conventional 34 W fluorescent lamp is  $\sim 30 : 1$ .

Replica molding permits the fabrication of microplasma devices in virtually any geometric pattern, and Fig. 8(b) is a photograph of a pattern of letters fabricated in  $200\text{-}\mu\text{m}$ -wide channels. In this structure, gas flow channels  $20 \mu\text{m}$  in width connect the letters, and since the plasma ignition voltage is a function of the channel width, delivering an rms voltage of 200 V to the array ignites only the letters in the array and not the interconnecting channels. The transparency of the array in Fig. 8(b) can also be seen by the reflection of the letter pattern from the rear face of the array structure.

#### IV. CONCLUSION

A replica molding process has been applied to the fabrication of microcavity plasma devices and arrays on both flexible polymer and rigid glass substrates. Microplasma pixels and channels can now be produced inexpensively and in virtually any pattern over surface areas of at least tens of square centimeters. These fully transparent arrays comprise plasma channels having widths as small as  $20 \mu\text{m}$  and aspect ratios as large as  $10^4 : 1$ . Operating voltages as low as 145 V (rms) have been observed for a driving voltage frequency of 20 kHz, and arrays incorporating a thin dielectric barrier film have been operated continuously for  $>24 \text{ h}$  with no noticeable degradation in performance. From these examples of microplasma array structures fabricated and tested thus far, it is clear that the ability to form plasma channels of complex shape in a transparent structure may prove of value for optical displays, plasma microreactors, and as a means for examining plasma-surface effects in a geometry in which the critical dimensions of the plasma region are approaching the Debye length.

#### ACKNOWLEDGMENT

The staff of the Micro and Nanotechnology Laboratory at the University of Illinois at Urbana-Champaign is gratefully acknowledged.

#### REFERENCES

- [1] D. L. Bitzer and H. G. Slottow, "The plasma display panel. a digitally addressable display with inherent memory," in *Proc. AFIPS Conf.*, 1966, vol. 29, pp. 541–547.
- [2] K. H. Becker, K. H. Schoenbach, and J. G. Eden, "Microplasmas and applications," *J. Phys. D*, vol. 39, pp. R55–R70, 2006.
- [3] M. J. Kushner, "Modeling of microdischarge devices: Pyramidal structures," *J. Appl. Phys.*, vol. 95, pp. 846–859, 2004.
- [4] J. G. Eden, S. J. Park, N. P. Ostrom, S. T. McCain, C. J. Wagner, B. A. Vojak, J. Chen, C. Liu, P. von Allmen, F. Zenhausern, D. J. Sadler, C. Jensen, D. L. Wilcox, and J. J. Ewing, "Microplasma devices fabricated in silicon, ceramic, and metal/polymer structures: Arrays, emitters and photodetectors," *J. Phys. D*, vol. 36, pp. 2869–2877, 2003.
- [5] S. J. Park, J. G. Eden, J. Chen, and C. Liu, "Microdischarge devices with 10 or 30  $\mu\text{m}$  square silicon cathode cavities: pd scaling and production of the XeO excimer," *Appl. Phys. Lett.*, vol. 85, pp. 4869–4871, 2004.
- [6] K. F. Chen, N. P. Ostrom, S. J. Park, and J. G. Eden, "One quarter million ( $500 \times 500$ ) pixel arrays of silicon microcavity plasma devices: Luminous efficacy above 6 lumens/watt with Ne/50% Xe mixtures and a green phosphor," *Appl. Phys. Lett.*, vol. 88, p. 061121, 2006.
- [7] J. Franzke, K. Kunze, M. Miclea, and K. Niemax, "Microplasmas for analytical spectrometry," *J. Anal. Atom. Spectrom.*, vol. 18, pp. 802–807, 2003.

- [8] S. J. Park, K. S. Kim, and J. G. Eden, "Ultraviolet emission intensity, visible luminance, and electrical characteristics of small arrays of Al/Al<sub>2</sub>O<sub>3</sub> microcavity plasma devices operating in Ar/N<sub>2</sub> or Ne at high-power loadings," *J. Appl. Phys.*, vol. 99, p. 026107, 2006.
- [9] —, "Nanoporous alumina as a dielectric for microcavity plasma devices: Multilayer Al/Al<sub>2</sub>O<sub>3</sub> structures," *Appl. Phys. Lett.*, vol. 86, p. 221501, 2005.
- [10] S.-J. Park, C. J. Wagner, C. M. Herring, and J. G. Eden, "Flexible microdischarge arrays: Metal/polymer devices," *Appl. Phys. Lett.*, vol. 77, pp. 199–201, 2000.
- [11] M. Bender, U. Plachetka, J. Ran, A. Fuchs, B. Vratzov, H. Kurz, T. Glinsner, and F. Lindner, "High resolution lithography with PDMS molds," *J. Vac. Sci. Technol. B*, vol. 22, pp. 3229–3232, 2004.
- [12] Y. N. Xia and G. M. Whitesides, "Soft lithography," *Angew. Chem.*, vol. 37, pp. 551–575, 1998.
- [13] B. T. Cunningham, P. Li, S. Schulz, B. Lin, C. Baird, J. Gerstenmaier, C. Genick, F. Wang, E. Fine, and L. Laing, "Label-free assays on the BIND system," *J. Biomolec. Screen.*, vol. 9, pp. 481–490, 2004.

**Meng Lu** (S'02) received the M.S. degree in electrical engineering from the University of Illinois at Urbana-Champaign in 2004, where he is currently pursuing the Ph.D. degree.

As a Master's student, he worked on electromagnetic simulation of surface plasma polarization waveguides. His current research focuses on the development of microfabrication techniques for display and biosensor applications.

**Sung-Jin Park** (M'01) received the M.S. and Ph.D. degrees in chemistry from Myongji University, Korea, in 1995 and 1999, respectively.

He worked in the areas of spectroscopy and organic and inorganic materials for applications in optoelectronics. In 1999, he joined the Laboratory for Optical Physics and Engineering, University of Illinois, as a Postdoctoral Research Associate. Between 2001 and 2003, he was with Ajou University, Korea, as a Professor Researcher. During that period, he studied nanostructured materials for flat lamp electrodes. In 2004, he became a Visiting Professor in the Department of Electrical and Computer Engineering, University of Illinois. His current research involves the study of microdischarge phenomena and the development of microplasma devices for photonics and display applications. He has more than 60 journal publications and holds 25 patents and patent applications.

Dr. Park is a member of the IEEE Lasers and Electro-Optics Society, the Sigma Xi Scientific Research Society, the American Chemical Society, and the Society for Information Display.

**Brian T. Cunningham** (M'00) received the B.S., M.S., and Ph.D. degrees in electrical and computer engineering from the University of Illinois at Urbana-Champaign.

He is an Associate Professor of electrical and computer engineering at the University of Illinois, where he is Director of the Nano Sensors Group. His group focuses on the development of photonic crystal-based transducers, plastic-based fabrication methods, and novel instrumentation approaches for label-free biodetection. He is a Founder and the Chief Technical Officer of SRU Biosystems, Woburn, MA, a life science tools company that provides high-sensitivity plastic-based optical biosensors, instrumentation, and software to the pharmaceutical, academic research, genomics, and proteomics communities. Prior to founding SRU Biosystems in June 2000, he was manager of Biomedical Technology at Draper Laboratory, Cambridge, MA, where he directed R&D projects aimed at utilizing defense-related technical capabilities for medical applications. In addition, he was Group Leader for MEMS Sensors at Draper Laboratory, where he directed a group performing applied research on microfabricated inertial sensors, acoustic sensors, optical switches, microfluidics, tissue engineering, and biosensors. Concurrently, he was an Associate Director of the Center for Innovative Minimally Invasive Therapy, a Boston-area medical technology consortium, where he led the Advanced Technology Team on microsensors. Before joining Draper Laboratory, he spent five years with the Raytheon Electronic Systems Division developing advanced infrared imaging array technology for defense and commercial applications. His thesis research was in the field of optoelectronics and compound semiconductor material science, where he contributed to the development of crystal growth techniques that are now widely used for manufacturing solid-state lasers and high-frequency amplifiers for wireless communication.

**J. Gary Eden** (S'75–M'76–SM'82–F'88) received the B.S. degree in electrical engineering (with high honors) from the University of Maryland, College Park, in 1972 and the M.S. and Ph.D. degrees from the University of Illinois at Urbana-Champaign in 1973 and 1976, respectively.

In 1976, he joined the Optical Sciences Division, U.S. Naval Research Laboratory, as a National Research Council Postdoctoral Associate, and from 1976 to 1979 was a Research Physicist in the Laser Physics Branch. He joined the faculty of the University of Illinois in 1979 and is currently Professor of electrical and computer engineering and Director of the Laboratory for Optical Physics and Engineering. At the University of Illinois, he has served as Associate Vice-Chancellor for Research, Associate Dean of the Graduate College, and Assistant Dean of Engineering. He has authored more than 200 journal publications and two books, and has received 22 patents.

Dr. Eden is a Fellow of the Optical Society of America and the American Physical Society. He received the IEEE Lasers and Electro-Optics Society (LEOS) Distinguished Service Award in 1996 and the IEEE Third Millennium medal in 2000. He was a LEOS Distinguished Lecturer for 2003–2005. He received the 2005 IEEE LEOS Aron Kressel Award. From 1996 to 2002, he was Editor-in-Chief of the IEEE JOURNAL OF QUANTUM ELECTRONICS and, in 1998, was President of LEOS.